Facilitated Tip-Positioning and Applications of Non-Electrode Tips in Scanning Electrochemical Microscopy Using a Shear Force Based Constant-Distance Mode

Andreas Hengstenberg,[a] Christine Kranz,[b] and Wolfgang Schuhmann*[a]

Dedicated to Prof. Dr. Hanns-Ludwig Schmidt, TU München, on the occasion of his 70th birthday

Abstract: In scanning electrochemical microscopy (SECM) a microelectrode is usually scanned over a sample without following topographic changes (constant-height mode). Therefore, deconvolution of effects from distance variations arising from non-flat sample surface and electrochemical surface properties is in general not possible. Using a shear force-based constant distance mode, information about the morphology of a sample and its localized electrochemical activity can be obtained simultaneously. The setup of the SECM with integrated constant-distance mode and its application to non-flat or tilted surfaces, as well as samples with three-dimensional surface structures are presented and discussed. The facilitated use of non-amperometric tips in SECM like enzyme-filled glass capillaries is demonstrated.

Keywords: constant-distance mode · enzyme capillaries · scanning probe microscopy · SECM · shear forces

Introduction

Scanning electrochemical microscopy (SECM) allows the derivation of topographic and chemical information about the surface of a sample from the Faraday current at an ultramicroelectrode (UME).[1–3] This current is determined by the deterioration of the hemispherical diffusion zone of a redox species in front of the UME, and the kinetics of a possible recycling of this redox species at the sample surface leading to a local increase of the concentration of the redox compound. Both effects are highly dependent on the tip-to-sample distance, however, with different functional relations. Furthermore, an additional dependence from the ratio of the UME radius to the size of its surrounding insulating shield[4] can be observed. A fundamental prerequisite for the unambiguous interpretation of SECM data is the knowledge of the tip-to-sample distance which allows to differentiate if a change in the UME current is caused by a variation in topography or an alteration of the local (electro)chemical reactivity.

[a] Prof. W. Schuhmann, Dr. A. Hengstenberg
Analytische Chemie, Elektroanalytik und Sensorik
Ruhr-Universität Bochum, 44780 Bochum (Germany)
Fax: (+49) 234-32-14683
E-mail: woschu@anachem.ruhr-uni-bochum.de

[b] Dr. C. Kranz
present address:
Institut für Analytische Chemie, Technische Universität Wien Getreidemarkt 9/151, 1070 Wien (Austria)

If the chemical nature of the sample surface varies locally the current at the UME cannot be used to establish a closed-loop feedback control maintaining constant tip-to-sample distance due to the different mechanisms which affect the UME current. A conducting spot surrounded by an insulator would cause this closed-loop feedback mechanism to decrease the electrode-to-sample distance resulting in a "tip crash". Therefore, most imaging performed so far with the SECM had been limited to flat sample surfaces with the UME scanned in a constant z position (constant-height mode). As a matter of fact, this imaging mode is only possible when changes of the sample height or the overall surface tilt do not exceed the tip-to-sample distance. Since the tip-to-sample distance has to be in the order of a few tip radii of the UME, it is obvious that with a decreasing electrode size scanning in this mode becomes more and more difficult.[5]

Two approaches to solve the problem have been reported so far. First, a feedback loop using the electrochemical approach curves in combination with a vertical modulation of the tip position,[6, 7] and second, the so-called "picking-mode" based on convective effects when the surface is approached by the UME with relative high speed.[8] Since both techniques are using the amperometric current through the UME for the determination of the tip-to-sample distance either normalized approach curves assuming a known ratio between electrode and shield diameter or tideous calibration procedures for each individual tip have to be applied. Especially in the case of the approach of the tip to insulating surfaces (negative feedback effect) the strong dependence of

 © WILEY-VCH Verlag GmbH, D-69451 Weinheim, 2000 0947-6539/00/0609-1547 $ 17.50+.50/0

the amperometric current from the ratio of the electrode radius to the surrounding insulator causes severe problems and prevents the application of these imaging modes for samples with high surface-activity variation and/or decreasing size of the UME.[4]

Due to the convolution of chemical and morphological information in the constant-height mode of the SECM the resolution, at least for non-flat surfaces, is not exclusively determined by the size of the UME. Since positive or negative feedback effects are obtained for distances between UME and sample surface which are in the order of the diameter of the UME (for extensive theoretical treatment see[4]) the aspect ratio of three-dimensional structures occurring on the sample surface represents an additional resolution determining parameter. Assuming, that the height of surface structures on the sample significantly exceeds the UME diameter and the tip positioning has been done over such a structure, the feedback distance will be lost while scanning over the surface. Thus, no localized information will be obtained for the rest of the surface. In contradistinction, when the tip positioning was performed within a valley in the surface structure, the tip will crash into the surface during the scan (Figure 1).

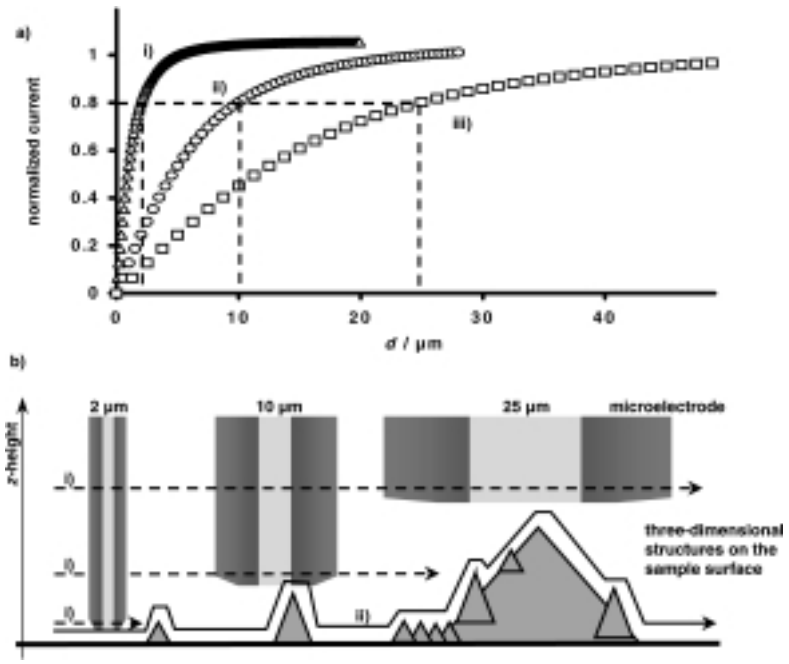

Figure 1. a) Approach curves assuming negative feedback calculated for UMEs with different active electrode size ($r = 12.5$ µm i), 5 µm ii) and 1 µm iii)) (calculated according to ref. [4] assuming a disk-to-insulating shield ratio of 1 to 10). The current decreases as the tip approaches an insulating surface, and hence a smaller electrode size leads to a decreased working distance. At a negative feedback current of 80 % of the diffusion-limited current in infinite distance the working distance equals approximately the active tip diameter. b) Using the active electrode diameter as working distance during lateral scanning electrodes will crash into three-dimensional surface structures with a height exceeding the working distance: i) shows the constant-height displacement leading to tip crash; ii) shows the optimal constant-distance displacement leading to improved resolution of three-dimensional surface structures and the deconvolution effects due to distance changes and changes of local chemical activity.

Additionally, since the distance dependence of the amperometric current is used as a source for the z positioning of the UME, new problems arise when non-amperometric tips are used in the SECM-experiment. Attempts to use potentiometric UMEs[9–11] or enzyme UMEs[12] have been reported. Severe problems for the exact positioning of such UMEs in close proximity to the sample surface avoiding a tip-crash have been described. Hence, whenever possible the determination of the distance was achieved by operating the electrode in an amperometric mode. For example double barrel electrodes which have one half of the tip working as an amperometric electrode and the other half as a separated potentiometric electrode have been developed to circumvent this problem.[13]

In scanning near-field optical microscopy (SNOM) shear force-based positioning of optical fiber tips had been described using optical detection systems,[14, 15] capacitance changes,[16] piezoelectric tuning forks,[17, 18] or piezoelectric detectors glued on a brass holder.[19] However, the application of most of these techniques in liquids is still extremely difficult. Recently, we have shown that a feedback mechanism relying on the detection of shear forces occurring between a vibrating UME and the sample surface can be successfully used in SECM.[20] A specially designed UME is vibrated at its resonance frequency using a piezoelectric tube for agitation.

Abstract in German: *In der elektrochemischen Rastermikroskopie (SECM) wird eine Ultramikroelektrode über eine Probenoberfläche gerastert, allerdings ohne dabei topographischen Änderungen zu verfolgen. Somit stellt das erhaltene Bild der Oberfläche eine Überlagerung des Einflusses der elektrochemischen Aktivität und dem Abstand zwischen Probenoberfläche und Mikroelektrode auf den gemessenen Faraday'schen Strom an der Mikroelektrode dar. Dies führt insbesondere bei dreidimensional strukturierten Oberflächen zu Fehlinterpretationen. Auf der Basis von Scherkraft-Wechselwirkungen zwischen einer in Resonanz schwingenden Mikroelektrode und der Probenoberfläche kann nun simultan die Morphologie der Probe und die lokale elektrochemische Aktivität aufgelöst werden. Der Aufbau eines SECM mit integrierter automatischer Repositionierung der Mikroelektrode auf der Basis der Detektion von Scherkraft-Wechselwirkungen sowie die Anwendung auf dreidimensional strukturierte oder relativ zur Rasterebene gekippte Oberflächen werden dargestellt. Weiterhin wird die mittels des Scherkraft-Modus vereinfachte Positionierung nicht-amperometrischer Abtastspitzen im SECM am Beispiel von Enzym-gefüllten Glaskapillaren demonstriert.*

 © WILEY-VCH Verlag GmbH, D-69451 Weinheim, 2000 0947-6539/00/0609-1548 $ 17.50+.50/0 *Chem. Eur. J.* **2000**, *6*, No. 9

A LASER beam is focused on the tip of the probe and the resulting Fresnel diffraction pattern is projected on a split photodiode. The vibration amplitude of the electrode can be monitored by phase-sensitive amplification of the difference signal of the split photodiode with respect to the agitation signal using a lock-in amplifier. In close proximity to the sample surface increasing shear forces lead to a damping of the vibration amplitude and a phase shift. Approach curves were presented, and the operation of the feedback loop during the electrochemical deposition of a polymer film has led to the formation of microscopic polymer towers which could be characterized using SECM in the constant-distance mode.[21] Very recently, a shear-force based constant-distance mode operated using a tuning fork resonance detection system[18] implemented in a commercially available SNOM has been successfully used in SECM-experiments to visualize the conductivity of a flat platinum microelectrode.[22]

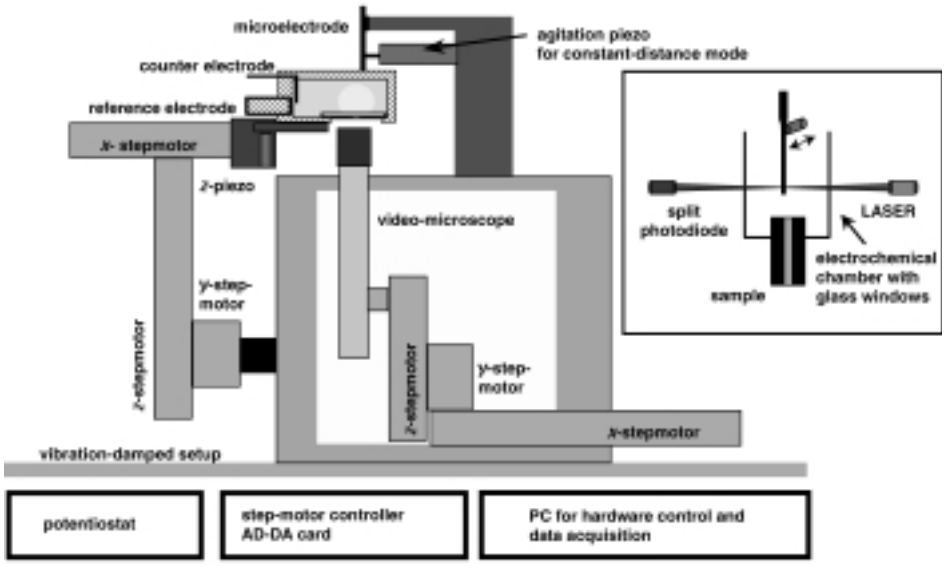

Figure 2. Schematic representation of the developed SECM set-up with integrated shear force-based constant distance mode. The sample is mounted on a *x*,*y*,*z* moving table. The electrode and the optical detection unit remain in a fixed position. A video microscope allows a bottom view through transparent samples. The inset shows in principle the electrochemical chamber equipped with glass windows as well as the alignment of the LASER and the split photodiode.

In this communication, we want to discuss possibilities to adapt the shear-force based constant-distance mode to a variety of different micro tips, facilitated tip-positioning, and three-dimensionally structured sample surfaces which could not be visualized previously using the conventional constant-height mode of the SECM.

Results and Discussion

Technical concept of a SECM with integrated shear-force-based distance control: In a conventional SECM apparatus images are obtained by scanning the tip electrode across the sample (the *x*,*y* plane) surface.[23] The integration of a shear-force based tip-positioning mode into a SECM leads to a number of presuppositions for the design of the set-up. Since a LASER beam has to be focused on the very end of the tip beneath the surface of the electrolyte, and typical agitation amplitudes for the vibrating tip are in the range of up to several nm, the tip position has to be kept in permanent alignment with the optical set-up. Thus, the tip holder with the agitation piezo, the laser, and the split photodiode have to be arranged on a rigid metal plate. As a consequence, the sample has to be moved in *x*,*y*,*z* direction under this fixed tip-position (Figure 2). Parallel glass windows in a specially designed electrochemical chamber made from polyacrylate, teflon or poly(chlorotrifluoroethylene), (KelF), allow the entrance and exit of the laser beam.

However, moving the sample together with the electrochemical chamber leads to changes of the insertion depth of the tip in the electrolyte solution with variations of the *z* height. It has to be assured that the damping of the amplitude of the vibrating tip is not or only little affected by the depth of insertion of the tip into the electrolyte. It was found that the vibration amplitude of the developed electrodes used for the presented studies is indeed dependent on the depth of insertion. However, this degree of damping occurring over the range of some mm was negligible as compared with the degree of damping that occurred upon final surface approach. Assuming three-dimensional surface structures with μm-dimensions the variation of the insertion depth of the micro-tip in the electrolyte is negligible with respect to the overall insertion depth of up to several mm.

Due to the extremely small agitation amplitude of the UME (see Experimental Section) no effect on the micro-electrode electrochemistry, for example, an increased current due to stirring effects, could be observed.

Shear force based distance determination in solution: As a consequence of the necessary agitation of the UME its vibration characteristics have to be evaluated and optimized in addition to its electrochemical properties. The UME consists of a Pt-wire sealed into a pulled glass capillary (see Experimental Section). In Figure 3, the resonance spectrum of such a glass capillary-based UME is shown. Usually, the resonance frequency leading to the highest resonance amplitude has been used for further investigations.

By changing the length of the vibrating tip of the UME and the diameter of the insulating sheath the resonance frequency can be adapted within a broad range, from 100 Hz up to at least 5 kHz.

The nature of the interaction mechanism leading to the shear forces between the vibrating tip and the sample surface is still a subject of discussion. The proposed interaction mechanisms include capillary forces, van der Waals forces[24]

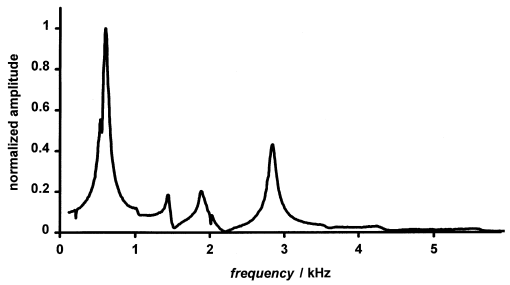

Figure 3. Vibration frequency spectrum of an electrode which has been developed for the shear force-based constant-distance mode. The spectra were taken with the tips immersed in water (approximate depth of 5 mm).

and direct mechanical contact.[25] Operated in liquid hydrodynamic forces are also expected to have a fundamental influence on the approach characteristics. This type of interaction depends on various parameters:

- *Morphology and physical properties of the sample surface*: The local structure of the surface determines the area of interaction with the UME. Soft surfaces can be deformed due to the force interactions.
- *Geometry and physical properties of the vibrating tip*: The area of interaction is additionally determined by the geometry of the UME. The physical properties of the UME material determine its spring constant and therefore its resonance frequency and vibration amplitude.
- *Viscosity of the electrolyte*: The composition and the temperature of the electrolyte determine the viscosity of the solution.

Due to these influences the approach behavior varies for each new electrode or sample. The vibration amplitude characteristics of an electrode approaching a gold covered glass surface have been compared in electrolytes with different viscosity. Care was taken to avoid any change in the fixation of the electrode or the sample. In Figure 4, two of these approach curves are shown. The shear-force induced damping occurs within a distance of about 100 nm from the surface. As expected for a hydrodynamic interaction mechanism, the distance dependence is correlated with the viscosity of the electrolyte.

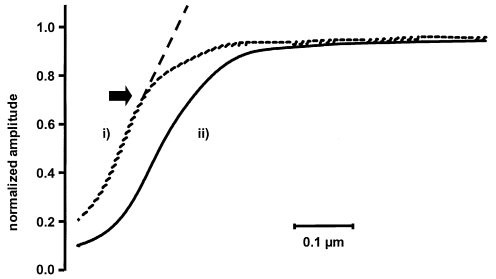

Figure 4. Amplitude-distance curves of a glass capillary-based UME in i) water and ii) a 1:1 water/glycerol mixture. The range of vibration damping is increased in a medium of higher viscosity. The approach was stopped, when the tip was lowered towards the surface to such an extend, that the resonance characteristics are lost (no lock-in signal). The set-point at 70% of the lock-in signal and the linear correlation function used as a basis for the software feedback loop for the re-positioning of the UME are shown.

Scanning flat surfaces: In the constant distance mode the amplitude of the vibrating UME is monitored and compared with a predefined value (set-point). Based on the resulting difference the distance between tip and sample is adjusted with the z positioning element using a feedback loop. The continuously maintained tip-to-sample distance of about 100 nm is very small as compared with the distances in conventional SECM-experiments using the constant-height mode. In constant-height mode imaging very often problems arise from the surface tilt of the sample relative to the x,y-raster plane leading eventually to a tip crash, especially if the initial distance has been chosen too small in order to obtain a maximal signal. Thus, for constant-height imaging it is indispensable to keep a rather large distance (at least in the first imaging experiment over an unknown sample) between UME and sample surface resulting in a loss of resolution. Thus, even for flat surfaces the developed constant-distance mode eliminates difficulties arising from a surface tilt leading to images with the best possible resolution due to a constant distance of only about 100 nm (Figure 5).

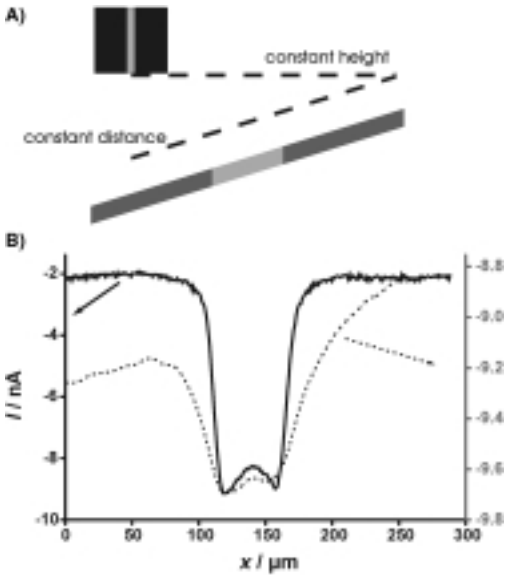

Figure 5. Constant-height and constant-distance imaging of a flat 50 µm diameter platinum electrode exhibiting a significant surface tilt. A) Schematic representation of the tip movement in the constant-height and the constant-distance mode. B) Line scans across the electrode. Left axis: constant-distance mode, right axis: constant-height mode. (10 mM $[Ru(NH_3)_6]^{3+}$ containing 100 mM KCl as electrolyte solution; UME at -300 mV versus Ag/AgCl, diameter of UME: 10 µm.)

Scanning surfaces with variations in topography: To evaluate the feasibility of the developed constant-distance mode for the visualization of the local electrochemical activity on three-dimensional surface structures, a model sample consisting of a Pt-wire of 10 µm diameter glued on a glass plate was chosen. Although this model sample seems to be an easy structure on the first sight, it integrates extremely big and immediate height changes overlaid with significant differences in the electrochemical surface activity. In order to evaluate the advantages of the shear-force based constant-distance mode over the conventional constant-height mode this sample structure was investigated using both imaging modes. In the

© WILEY-VCH Verlag GmbH, D-69451 Weinheim, 2000
0947-6539/00/0609-1550 $ 17.50+.50/0 *Chem. Eur. J.* **2000**, *6*, No. 9

constant-distance mode the current obtained due to the reduction of $[Ru(NH_3)_6]^{3+}$ and the z position at constant amplitude damping have been recorded simultaneously (Figure 6i, ii), while in the constant-height mode only the UME current was recorded (Figure 6iii).

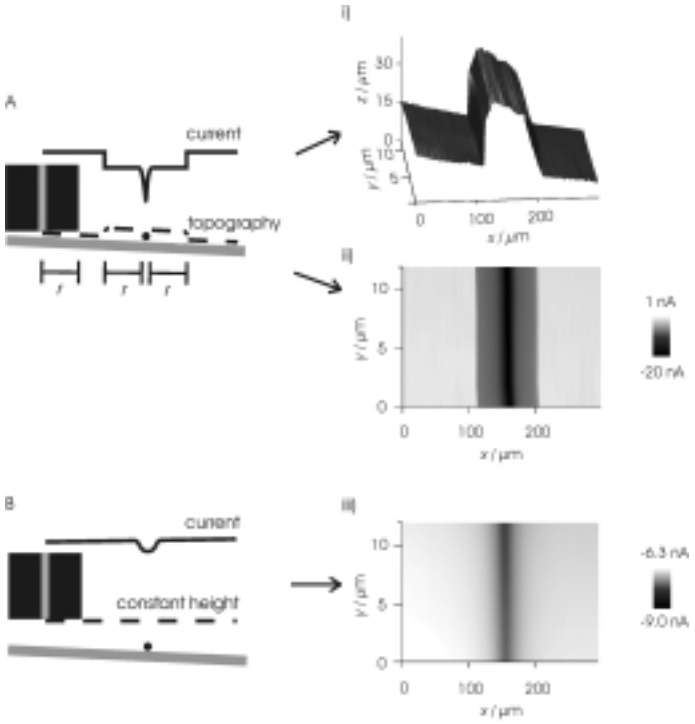

Figure 6. Constant-height and constant-distance imaging of a 10 µm diameter platinum wire glued onto a glass slide. A) Schematic representation of the shear-force based constant-distance mode leading simultaneously to a i) topographical and ii) a current image of the sample. B) Schematic representation of the constant-height mode and the iii) obtained current image. (5 mM $[Ru(NH_3)_6]^{3+}$ containing 100 mM KCl as electrolyte solution; UME at -300 mV versus Ag/AgCl, diameter of UME: 10 µm).

Obviously, the developed constant-distance mode is able to reposition the UME even over the extremely steep and sudden height differences of the structure. As common for all scanning-probe techniques,[26, 27] the topographic image represents a convolution between sample and tip geometry. Thus, the observed width of 96 µm for the Pt-wire is determined by the features of the Pt-wire itself (10 µm) plus the width of the vibrating micro-tip which was about 85 µm (electrode disk with insulating sheath). The z position of the UME is starting to increase, when the side of the vibrating tip is "sensing" the Pt-wire. Simultaneously, the reduction current (negative feedback over the non-conducting glass surface) is increasing due to the better diffusional access of the Ru-complex to the UME (see schematic drawing in Figure 6A). When the active electrode area of the UME is directly positioned over the Pt-wire, the reduction current is increasing to about 20 nA due to the positive feedback effect. Although, the topographic image represents the mentioned convolution between tip and sample geometry, the observed positive feedback current is sensing the electrochemically active surface with high resolution (width at half height of 13 µm) due to the extremely close distance between UME and sample surface.

In contrast, using the constant-height mode with a similar small distance of 100 nm between UME and the sample would lead to a crash of the tip into the Pt-wire (Figure 6B). Thus, expecting three-dimensional surface structures with high aspect ratio, the surface approach has to be stopped at a bigger distance. Scanning over the Pt-wire in a z height (e.g., 70% of the current in infinite distance during the approach of the non-conducting glass surface) leads to a current difference of only 3.3 nA between the negative feedback over the glass surface and the positive feedback over the platinum wire. Additionally, no information concerning the sample tilt is obtained in this mode as compared with the topographical image obtained using the constant-distance mode (Figure 7). Moreover, the decreased sensitivity in the constant-height mode leads to a significant loss of resolution with a width at half height of about 32 µm detected for the 10 µm Pt-wire (Figure 6iii).

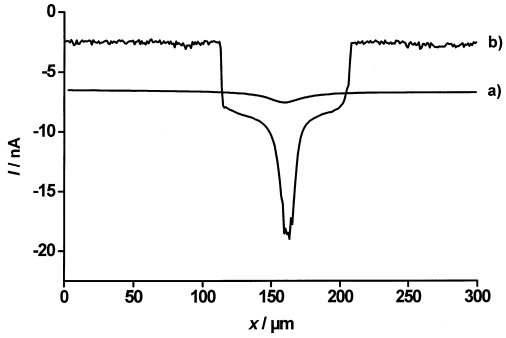

Figure 7. Comparison of two line scans across a 10 µm diameter platinum wire (same structure than in Figure 6). a) constant-height mode, b) shear-force based constant-distance mode (experimental parameters: see Figure 6).

Enzyme-filled capillaries as an example for non-electrode tips: In order to demonstrate the feasibility of the developed constant-distance mode to circumvent positioning problems which occurred previously with non-amperometric tips, we have investigated the application of enzyme-filled glass capillaries in SECM (Figure 8). The glass capillaries have been filled with a polymer hydrogel containing either glucose

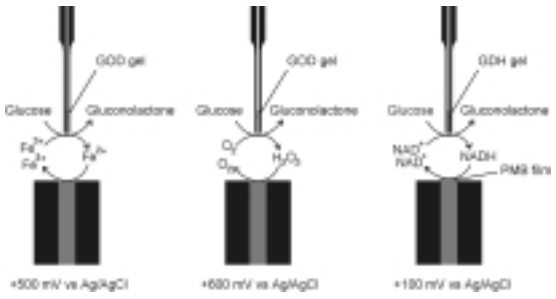

Figure 8. Principles of generation collection experiments with enzyme filled glass capillaries. The enzyme generates a redox species (left: Fe^{2+}, middle: H_2O_2, right: NADH) which then diffuses to the substrate electrode at which it is converted at an appropriate potential. The current through the substrate electrode is used as information to visualize the local chemical activity with respect to the x,y position of the enzyme tip.

oxidase or glucose dehydrogenase as biocatalysts. These enzyme capillaries have been positioned over a 50 μm Pt-electrode in the case of glucose oxidase, and over a poly-(methylene blue)-modified microelectrode[28] in the case of the glucose-dehydrogenase capillary. The enzymatic reaction which is localized to the very end of the tip is used for the generation of redox species which may be detected at the sample surface in dependence of its local activity. With the glucose-oxidase tip, H_2O_2 and $[Fe(CN)_6]^{3-}$ have been used as free-diffusing redox species. In the first case, H_2O_2 is generated at the enzyme tip in the presence of glucose and O_2. The locally generated H_2O_2 diffuses to the perpendicular positioned Pt-microelectrode where it is oxidized at an applied potential of 600 mV versus Ag/AgCl.

Using instead the $[Fe(CN)_6]^{3-}/[Fe(CN)_6]^{4-}$ redox couple as artificial redox mediator for the regeneration of the intermediately reduced glucose oxidase, the perpendicular positioned Pt-microelectrode has to be poised to a potential sufficient to oxidize $[Fe(CN)_6]^{4-}$. In the absence of glucose no electrochemical conversion occurs at the Pt-electrode. After addition of a saturation concentration of glucose, $[Fe(CN)_6]^{3-}$ acts as electron acceptor for the reduced enzyme and $[Fe(CN)_6]^{4-}$ is generated at the enzyme tip in proportion to the enzymatic oxidation of glucose. The Pt-electrode serves as collector for these enzymatically reduced species, and their re-oxidation leads to a current which can be used to identify the surface activity of the sample (Figure 9a).

In a similar way a glucose dehydrogenase-filled capillary can be applied to obtain information about the catalytic activity of a modified electrode surface. It is known that poly(methylene blue) films are catalytically active to oxidize NADH at a low working potential,[28] however, until now only an integral activity averaged over the entire surface of the modified electrode surface could be measured. In order to visualize locally this catalytic activity, NADH has to be generated with a defined rate at a spatially limited spot. In the presence of glucose and NAD^+, both in saturation concentrations, NADH is generated at the glucose dehydrogenase tip with a defined rate constant. The poly(methylene blue)-modified microelectrode is used as collector electrode poised to a potential of 100 mV versus Ag/AgCl to enable catalytic NADH oxidation. The catalytic surface activity can be clearly visualized (Figure 9b) and the homogeneity of the catalytic activity can be monitored with the resolution determined by the size of the glucose-dehydrogenase tip.

This situation is similar to the tip generator/substrate collector arrangement, which allows to perform generation/collection experiments with high collection efficiency.[29] However, using the constant-distance mode together with (bio)catalytic-active non-electrode tips may extend the application of this mode to locally generated species which are not accessible by electrochemical processes. Thus, the possibility to accurately position non-electrode tips over rough sample surfaces will open the field for the local investigation of specific surface reactions defined by the species generated at the tip using inorganic catalysts, biocatalysts, or electrochemical techniques.

Conclusion

The presented studies show how a closed feedback loop relying on the detection of shear forces between a vibrating tip and the sample surface extend the experimental applications of SECM towards the investigation of rough or tilted samples, generation collection experiments with non-electrode tips and facilitated tip positioning avoiding tip crash. The ability of keeping a constant distance by means of a shear-force controlled feedback loop while scanning over a sample will allow to use tips with decreased size and thus enhance the resolution obtained from the investigation of non-flat sample surfaces.

It has been demonstrated that a LASER based shear-force detection scheme can be used successfully in liquids. Since there are no physical connections between the vibrating UME and the laser-based detection system the size, stiffness, and resonance behavior of the UMEs can be varied in a wide range. In contrast, the recently introduced tuning-fork positioning[22] is laser-free and should offer some advantages with respect of the design of the necessary measuring chambers and the basic set-up of the system. However, severe restrictions concerning electrode size, geometry and vibrational properties are encountered due to the convolution of the tip vibration with the resonance frequencies of the simultaneously vibrating electrode holder.

Generation collection experiments have been carried out with enzyme modified tips. The experiments demonstrate new methods for the characterization and imaging of sensor surfaces. Compounds like NADH which can not be generated using electrochemical methods are now available for generation-collection experiments allowing a more detailed study of immobilized enzymes, their stability and their reactivity with different mediating substances. Additionally, the

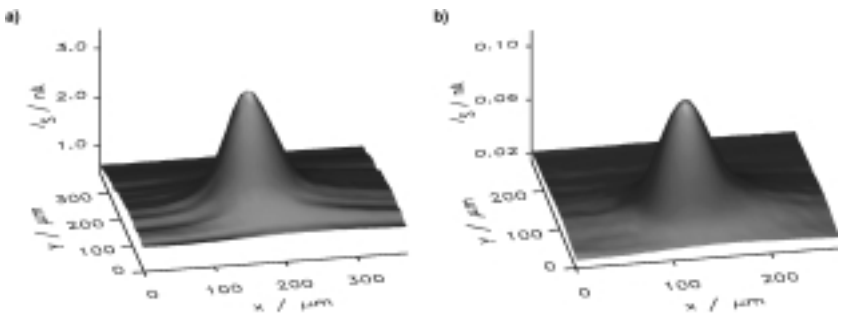

Figure 9. Identification of reactive spots with enzyme-filled capillaries. a) Image of a 50 μm diameter platinum electrode obtained with glucose oxidase modified capillary tip. (50 mM glucose in 100 mM phosphate buffer pH 7.0 containing 20 mM $K_3[Fe(CN)_6]$). b) Image of a 50 μm poly(methylene blue)-modified platinum electrode using enzymatically generated NADH as redox mediator. The NADH was generated at the glucose dehydrogenase-modified capillary tip in a solution containing 50 mM glucose and 10 mM NAD^+ in a 100 mM phosphate buffer pH 7.0.

© WILEY-VCH Verlag GmbH, D-69451 Weinheim, 2000
0947-6539/00/0609-1552 $ 17.50+.50/0 *Chem. Eur. J.* **2000**, *6*, No. 9

surface approach by means of the shear-force mechanism should facilitate the use of tips that do not show an intrinsic distance dependent signal. This might become significant for pH microscopy and the use of ion-sensitive tips. The possibility to image complex three-dimensional structures in SECM may lead to new applications of micro-electrochemistry. Corresponding studies are in progress.

Experimental Section

Instrumentation

SECM-components: A LASER (CDM 14S/S70/1 Atos, Pfungstadt, Germany) and a split photodiode (Spot 4D, LASER 2000, Weßling, Germany) are mounted on micrometer-screw driven positioning tables (OWIS, Staufen, Germany) for fine adjustments. The difference signal of the split photodiode is preamplified with a home-built difference amplifier and then fed into the signal input of a lock-in amplifier (Princeton Applied Research, Model 5210, EG&G, Bad Wildbad, Germany). A piezo tube is connected to the electrode holder via a flexible metal blade, which can be slightly bend to press the piezo tube to the electrode shaft. Using the built-in oscillator of the lock-in amplifier a sinusoidal voltage of up to 2 V can be applied to a piezo tube (PST500/5/15, Piezomechanik Pickelmann, München, Germany) with 15 μm maximal displacement at 500 V. Agitation of the micro-tip has been performed with amplitudes of up to 60 nm. However, much smaller amplitudes are possible,[20] and typical amplitudes of about 100 mV corresponding to about 3 nm are used.

The electrochemical chamber with the sample is mounted on a *x*,*y*,*z*-positioning stage driven by computer controlled stepper-motors having a nominal resolution of 10 nm per micro-step (SPI Robot Systeme, Oppenheim, Germany). For a fast control of the *z* height in a closed-loop feedback control an additional piezo-driven displacement table has been used (Owis, Staufen, Germany); maximal displacement 200 μm at 500 V).

The electrochemical chamber made from polyacrylate, teflon, or KelF is equipped with parallel aligned glass windows allowing the LASER beam to pass through the electrolyte. The electrochemical chamber is completed by an Ag/AgCl/3 M Cl^- reference electrode (Biometra, Göttingen, Germany) and a platinum wire auxiliary electrode. The bottom of the measuring chamber can be easily exchanged in order to facilitate the integration of different samples (e.g., modified electrodes with different diameters, flat structures, or a transparent glass substrate). For transparent samples and to facilitate tip approach and object finding a video microscope (optical resolution approx. 5 μm) is integrated into the set up. A BAS petite ampere potentiostat (BAS, West Lafayette, USA) was used for amperometric measurements. Cyclic voltammetry was performed with a in-house-built potentiostat. The system was controlled using a personal computer equipped with a standard data acquisition board (CIODAS 1602, PlugIn Instruments, Eichenau, Germany) and a in-house-written Windows software in Microsoft Visual Basic 3.0 (Microsoft, Redmont, USA).

Electrode preparation

Glass-insulated platinum electrodes: The end of a borosilicate glass capillary (Art.-Nr. 14 003 72, Hilgenberg, Hilgenberg, Germany) was drawn with a in-house-built puller to a hollow fiber of 1 – 1.5 cm length. A 25 μm or 10 μm-diameter platinum wire (Goodfellow, Cambridge, UK) was inserted and then sealed under vacuum into the fiber using a heating coil. The resulting pipette was inserted into a conventional Pasteur pipette which is cut according to the length of the fiber. Parts of the assembly were filled with a resin normally used in optical industry (Rodenstock, München, Germany) in order to stabilize the fragile fiber for grinding and polishing. Fine sandpaper was used for grinding until the platinum disk was exposed. The ratio of insulator thickness to the Pt-wire radius varied between 5 – 10 according to different pulling parameters of the glass capillary. After polishing with 3, 1 and 0.5 μm alumina paste the resin was removed with acetone and the electrode taken out of the Pasteur pipette and contacted with a copper wire and silver epoxy glue (H20, EpoTek, Waldbronn, Germany).

Enzyme tips: As described above hollow-fiber capillaries with a tip opening of 10 μm (estimated with light microscopy) were prepared. If necessary they were grounded and polished to obtain a smooth opening. They were filled with a mixture of an aqueous poly(vinylacetate)-poly(ethylene)-co-polymer dispersion (Vinnapas EP16, Wacker, Burghausen, Germany) with enzyme dissolved in buffer.[30] The mixture contained 2 mg of enzyme (either glucose oxidase from *Aspergillus niger*, EC 1.1.3.4., grade VII S, Sigma, Deisenhofen, Germany or glucose dehydrogenase from *Bacillum megaterium*, EC 1.1.1.47, Merck, Darmstadt, Germany) dissolved in 10 μL buffer per 25 mg polymer dispersion. The tips were allowed to dry overnight in the refrigerator before use.

Samples: Poly(methylene blue)-modified platinum electrodes were prepared by electrochemical polymerization from a degassed 2.5 mM solution of methylene blue (Merck, Darmstadt, Germany) in 100 mM borate buffer (pH 9.1) containing 100 mM KCl following a procedure described previously.[28] They were cycled 10 times between −450 mV and +1200 mV versus Ag/AgCl with a scan rate of 100 mV s^{-1}. After polymerization the electrode surface was rinsed with buffer and kept in buffer at room temperature. NADH was oxidized at an applied working potential of +300 mV versus Ag/AgCl.

Imaging in the constant-distance mode: For the shear-force detection the oscillator of the lock-in amplifier was tuned to the resonance frequency of the tip immersed in the electrolyte. Prior to the start of the imaging procedure the feedback loop for repositioning of the microelectrode has to be established. The measuring chamber with the sample is slowly approached to the vibrating tip concomitantly monitoring the vibration amplitude (final approach speed 0.2 μm s^{-1}). The vibration amplitude in dependence from the *z* position is graphically displayed on the screen. The *z* approach is stopped automatically at a predefined degree of damping of the vibration amplitude of the tip (e.g. 70 % of the undamped value which is called "set-point" in the following description). The software then allows to determine the slope at the end of the approach curve (see Figure 4). This derivative defines a linear function between the damping of the vibration amplitude and the displacement in *z* direction, which is then used to determine the sensitivity of the closed-loop feedback control. Such a feedback loop usually tends to over-swing around the set-point, especially when the feedback loop is too sensitive with a significant noise level. By means of a damping factor, which can be chosen freely, the over-swinging can be reduced. Obviously, this damping factor delays the response of the system to changes in the morphology. Thus, by means of a proper setting of this damping factor it has to be assured that the damping does not lead to a poor and slow response to changes in the topography of the sample. After optimization the imaging can be started (usually a speed of 0.88 μm s^{-1} was used for the *x* and *y* displacement with unknown sample morphology expecting structures with high aspect ratio) while in the background the established feedback loop is adjusting the constant tip-to-sample distance. In principal, the software allows to choose between two options. Either, the sequential steps of the imaging mode (incremental displacement, equilibration time, measurement of the current) or the proper *z* positioning control via the closed feedback loop define the time course of the experiment.

Acknowledgement

The helpful input of the workshop staff at the Department of Chemistry of the Ruhr-Universität Bochum, especially by Armin Lindner, during the set-up of the described SECM is gratefully acknowledged.

[1] A. J. Bard, F. F. Fan, D. T. Pierce, P. R. Unwin, D. O. Wipf, F. Zhou, *Science* **1991**, *253*, 68.
[2] A. J. Bard, F. F. Fan, J. Kwak, O. Lev, *Anal. Chem.* **1989**, *61*, 132.
[3] R. C. Engstrom, C. M. Pharr, *Anal. Chem.* **1989**, *61*, A1099.
[4] J. Kwak, A. J. Bard, *Anal. Chem.* **1989**, *61*, 1221.
[5] Y. Shao, M. V. Mirkin, G. Fish, S. Kokotov, D. Palanker, A. Lewis, *Anal. Chem.* **1997**, *69*, 1627.
[6] D. O. Wipf, A. J. Bard, *Anal. Chem.* **1992**, *64*, 1362.
[7] D. O. Wipf, A. J. Bard, D. E. Tallman, *Anal. Chem.* **1993**, *65*, 1373.
[8] K. Borgwarth, D. Ebling, J. Heinze, *Ber. Bunsenges. Phys. Chem.* **1994**, *98*, 1317.

[9] G. Denuault, M. H. T. Frank, L. M. Peter, *Faraday Discuss.* **1992**, 23.
[10] C. Wei, A. J. Bard, G. Nagy, K. Toth, *Anal. Chem.* **1995**, *67*, 1346.
[11] B. J. Horrocks, M. V. Mirkin, D. T. Pierce, A. J. Bard, G. Nagy, K. Toth, *Anal. Chem.* **1993**, *65*, 1213.
[12] B. R. Horrocks, D. Schmidtke, A. Heller, A. J. Bard, *Anal. Chem.* **1993**, *65*, 3605.
[13] C. Wei, A. J. Bard, I. Kapui, G. Nagy, K. Toth *Anal. Chem.* **1996**, *68*, 2651.
[14] E. Betzig, P. L. Finn, J. S. Weiner, *Appl. Phys. Lett.* **1992**, *60*, 2484.
[15] E. Betzig, J. K. Trautman, T. D. Harris, J. S. Weiner, R. L. Kostelak, *Science* **1991**, *251*, 1468.
[16] M. Lee, E. B. McDaniel, J. P. Hsu, *Rev. Sci. Instr.* **1996**, *67*, 1468.
[17] R. D. Grober, K. Karrai, *Appl. Phys. Lett.* **1995**, *66*, 1842.
[18] R. D. Grober, K. Karrai, *Ultramicroscopy* **1995**, *61*, 197.
[19] R. Brunner, A. Bietsch, O. Hollricher, O. Marti, *Rev. Sci. Instr.* **1997**, *68*, 1769.
[20] M. Ludwig, C. Kranz, W. Schuhmann, H. E. Gaub, *Rev. Sci. Instr.* **1995**, *66*, 2857.
[21] C. Kranz, H. E. Gaub, W. Schuhmann, *Adv. Mater.* **1996**, *8*, 634.
[22] P. I. James, L. F. Garfias-Mesias, P. J. Moyer, W. H. Smyrl, *J. Electrochem. Soc.* **1998**, *145*, L64.
[23] J. Kwak, A. J. Bard, *Anal. Chem.* **1989**, *61*, 1794.
[24] R. Toledo-Crow, P. C. Yang, Y. Chen, M. Vaez-Iravani, *Appl. Phys. Lett.* **1992**, *60*, 2957.
[25] M. J. Gregor, P. G. Blome, J. Schöfer, R. G. Ulbrich, *Appl. Phys. Lett.* **1992**, *68*, 307.
[26] J. E. Griffith, D. A. Grigg, M. J. Vasile, P. E. Russell, E. A. Fitzgerald, *J. Vacuum Sci. Technol. B* **1991**, *9*, 3586.
[27] L. Montelius, J. O. Tegenfeldt, *Appl. Phys. Lett.* **1993**, *62*, 2628.
[28] A. A. Karyakin, E. E. Karyakina, W. Schuhmann, H.-L. Schmidt, S. D. Varfolomeyev, *Electroanal.* **1994**, *6*, 821.
[29] C. Lee, J. Kwak, F. C. Anson, *Anal. Chem.* **1991**, *63*, 1501.
[30] J. Popp, A. Silber, C. Bräuchle, N. Hampp, *Biosens. Bioelec.* **1995**, *10*, 243.

Received: October 15, 1999 [F2094]

© WILEY-VCH Verlag GmbH, D-69451 Weinheim, 2000
0947-6539/00/0609-1554 $ 17.50+.50/0